Petroleum Science 22 (2025) 909–924

Contents lists available at ScienceDirect

Petroleum Science

journal homepage: www.keaipublishing.com/en/journals/petroleum-science

Original Paper

Feasibility study of a process for the reduction of sulfur oxides in flue gas of fluid catalytic cracking unit using the riser reactor

Fa-Lu Dang [a], Gang Wang [a, *], Jing-Cun Lian [a], Yu Yang [a, b], Mei-Jia Liu [a]

[a] State Key Laboratory of Heavy Oil Processing, College of Chemical Engineering and and Environment, China University of Petroleum, Beijing, 102249, China
[b] State Key Joint Laboratory of Environment Simulation and Pollution Control, School of Environment, Tsinghua University, Beijing, 100084, China

ARTICLE INFO

Article history:
Received 28 March 2024
Received in revised form
18 September 2024
Accepted 25 September 2024
Available online 27 September 2024

Edited by Min Li

Keywords:
Sulfur oxides
New catalytic cracking process
Thermodynamic analysis
Kinetic analysis
Sulfur recovery

ABSTRACT

In this work, a new process for achieving the recovery of elemental sulfur by utilizing a fluidized catalytic cracking (FCC) riser reactor for SO_x treatment (FCC-DeSO_x) is proposed. The process leverages the high temperatures and hydrocarbon concentrations in the FCC riser reactor to convert SO_x into H_2S. Subsequently, H_2S, along with the cracked gas, is processed downstream to produce sulfur. Thermodynamic analysis of the key reduction reactions in the FCC-DeSO_x process revealed that complete conversion of SO_x to H_2S is feasible in the dry gas (hydrogen-rich) prelift zone, as well as the upper and lower zones of the riser, upon achieving thermodynamic equilibrium. Experimental studies were conducted to replicate the conditions of these reaction zones using a low concentration of hydrogen gas as the reducing agent. Through process optimization, investigation of the minimum reaction time, and kinetic studies, the potential of this method for the complete reduction of SO_x was further confirmed.
© 2024 The Authors. Publishing services by Elsevier B.V. on behalf of KeAi Communications Co. Ltd. This is an open access article under the CC BY-NC-ND license (http://creativecommons.org/licenses/by-nc-nd/4.0/).

1. Introduction

Fluid catalytic cracking (FCC) is the primary process used to refine heavy and crude oils and produce light olefins in the petroleum industry (Corma et al., 2017; Alotaibi et al., 2018; Xu et al., 2021; Oloruntoba et al., 2022; Stratiev et al., 2023). In the FCC reaction-regeneration process, sulfur in the feedstock partially enters the coke and is deposited on the catalyst in the reactor, subsequently the coke on the catalyst is burned in the regenerator to generate SO_x-containing flue gas, elemental sulfur in the FCC flue gas accounts for 5%–15% of the total sulfur in the feedstock (Hu, 2012). The SO_x concentration in the FCC regeneration flue gas reaches 0.015–0.3 v% (Li, 2017), and its SO_x emissions reach 10–420 thousand tonnes/year, which is a significant contributor to sulfur oxide (SO_x) emissions in refining industry (Chen and Xu, 2015; Gong, 2020; Luan et al., 2020). As the quality of FCC feedstocks decreases, the amount of SO_x in the flue gas increases (Cheng et al., 2009; Li and Yuan, 2014; Wu, 2021; Li et al., 2022). Efforts have been made to develop FCC flue gas desulfurization technology to efficiently remove SO_x (Chen and Weng, 2005; Feng et al., 2016). Typical flue gas desulfurization technologies such as sodium hydroxide, calcium carbonate or amine absorption method, are based on acid-alkali absorption principles, but often overlook the potential resource utilization of SO_x (Chen et al., 2020; Li et al., 2020; Liu et al., 2020; Nie et al., 2020; Wang et al., 2020; Gong, 2022). By achieving emission reduction of industrial waste and effectively utilizing SO_x resources through process technology innovation, we can not only meet stringent Chinese SO_x emission standards (GB 31571-32015), but also generate significant economic benefits (Magnabosco, 2007; Zhao et al., 2022; Ge et al., 2023; Huang, 2023).

The ultimate goal in resource utilization is to convert SO_x into sulfur (Zhou, 2020; Li, 2023), an easily storable compound that serves as a primary feedstock for various products. Every refinery requires a sulfur recovery unit to extract H_2S from FCC cracked gas. Effectively converting SO_x to H_2S from FCC flue gas can enhance the feedstock supply for the sulfur unit and improve overall economic efficiency.

In response to the technical challenges faced in reducing SO_x emissions in FCC flue gas, numerous scholars have investigated the use of sulfur transfer agents (Polato et al., 2008; Baillie, 2019). These agents facilitate the sulfate formation during the regeneration of FCC catalysts, which are subsequently reduced to H_2S by hydrocarbons in the FCC reactor. H_2S can then be directed to the Claus unit to produce sulfur (Polato et al., 2005; Jiang et al., 2011; Feng et al., 2014; Gaudin et al., 2016; Jiang et al., 2016; Yi and Ma,

* Corresponding author.
E-mail address: wanggang@cup.edu.cn (G. Wang).

https://doi.org/10.1016/j.petsci.2024.09.021
1995-8226/© 2024 The Authors. Publishing services by Elsevier B.V. on behalf of KeAi Communications Co. Ltd. This is an open access article under the CC BY-NC-ND license (http://creativecommons.org/licenses/by-nc-nd/4.0/).

2019). However, the sulfur transfer agent is alkaline and it reduces heavy oil conversion, so it is below 5 wt% of the FCC catalyst usage, which results in less than 80% SO_x removal rate of FCC flue gas. Other scholars have explored various catalysts for SO_x reduction in FCC flue gas, Al_2O_3-loaded transition metal sulfides, rare-earth oxides, and chalcocite-type catalysts, to reduce SO_x to H_2S and sulfur (Mirhoseini and Taghdiri, 2016; Zhang et al., 2016; Hou et al., 2017; Miao and Dutta, 2017; Xia et al., 2017; Ge et al., 2018; Mousavi et al., 2018). Nevertheless, these catalysts still face challenges such as poor resistance to oxygen and rapid deactivation, which hinder the development of desulfurization technology for oxygenated FCC flue gas.

To address these challenges and achieve efficient utilization of SO_x in FCC flue gas, we propose a novel process called FCC-DeSO_x, which utilizes an FCC riser reactor. As illustrated in Fig. 1, the flue gas undergoes pretreatment, such as flue gas purification with activated carbon (Olson et al., 2000; Humeres et al., 2002; Bejarano et al., 2003; Zawadzki and Wisniewski, 2007), the key reactions of flue gas pretreatment are shown in Table 1, the process removes NO_x, fine catalyst particulates, and oxygen, furthermore convert SO_3 to SO_2, resulting in SO_x-rich gas (SO_2/SO_3 molar ratio>100). By further utilizing the FCC riser reactor, along with a prelift of dry gas (rich in hydrogen), a high reaction temperature, and high concentrations of hydrogen or hydrocarbons, SO_2-rich gas can be reduced to H_2S. The resulting H_2S is then directed to downstream processes to generate sulfur products, thereby achieving the goal of treating SO_x waste gas using existing units and ensuring the recovery of sulfur from the sulfurous gas.

This paper investigates the limitations imposed by thermodynamic equilibrium on the reduction reactions between SO_2 and SO_3 with petroleum hydrocarbons, hydrogen, and catalysts during the FCC process. By comparing the thermodynamic equilibrium concentrations of various reactions, the equilibrium limitations in reducing SO_x to H_2S are determined, providing theoretical support for process development. Subsequently, a feasibility study is conducted, which includes process optimization, exploration of the shortest reaction time, and kinetic modeling using a small tubular reactor to simulate the catalytic cracking environment in the riser. The feedstock consists of a mixture of SO_2 and N_2, with a low concentration of hydrogen (H_2) serving as the reducing gas.

2. Computational and experimental

2.1. Thermodynamic computational methods

The key to realizing the industrial application of FCC-DeSO_x technology is the complete conversion of SO_x to H_2S. Residual SO_x and H_2S can react to form sulfur in high-temperature transport pipelines, leading to clogged pipelines and plant shutdowns. Additionally, SO_3 can react with Al_2O_3, the main component of the catalyst, to form sulfate under the FCC reaction environment, which can affect the catalyst's properties. Therefore, it is necessary to study the thermodynamic equilibrium limits of the reduction reactions occurring between SO_2 and SO_3 with petroleum hydrocarbons, hydrogen, and catalysts during the FCC process. This study aimed to reduce the impact of the SO_x reduction reaction on the properties of FCC products and catalysts and to provide theoretical support for process development.

The thermodynamic reaction network for the reduction of SO_x in the riser was calculated to obtain the free energy, equilibrium constant, equilibrium conversion, and thermodynamic equilibrium concentration variation rule with temperature for the reduction of SO_x to H_2S or S_2 under FCC conditions for different reductants. Thermodynamic computational analysis was performed using HSC Chemistry software, which includes thermodynamic data for more than 20,000 substances. The calculations are based on the principle of Gibbs free energy minimization, and the product distributions are determined by minimizing the Gibbs free energy based on the reactions involved in the reaction system. The equations for the Gibbs free energy of the reaction (Δ_rG_m) and the reaction equilibrium constant (k) derived from the HSC Chemistry software are shown as:

$$\Delta_rG_m = \sum \mu \Delta_rG_f \tag{1}$$

$$k = \exp\left(\frac{-\Delta rGm}{RT}\right) \tag{2}$$

Where Δ_rG_f is the standard molar Gibbs free energy of generation at the reaction temperature, kJ/mol; Δ_rG_m is the standard molar Gibbs free energy of reaction at the reaction temperature, kJ/mol, respectively; μ is the reaction stoichiometry; k is the standard equilibrium constant of the chemical reaction; R is the gas constant, J/(mol·K); and T is the reaction temperature, K.

2.2. Experimental procedure and product analysis

2.2.1. Feedstock and catalyst

Four types of standard gases were used in the SO_2 reduction experiments, include H_2 (6.0 v% hydrogen), SO_2 (1.0 v% SO_2), CH_4 and C_2H_6 (4.5 v% methane and 1.5 v% ethane), H_2, CH_4 and C_2H_6 (6.0 v% hydrogen, 4.5 v% methane and 1.5 v% ethane) standard gases

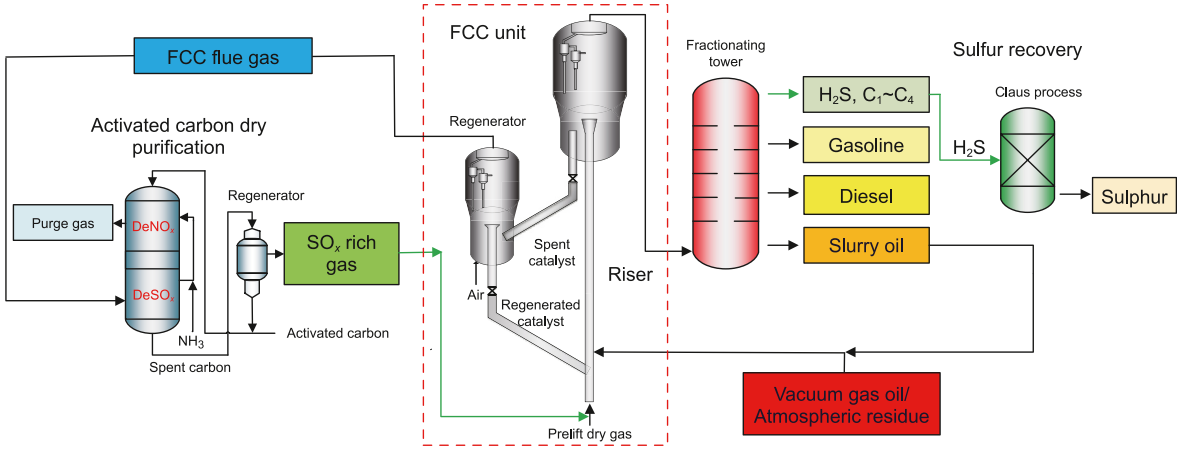


Fig. 1. Schematic diagram of the process of treating SO_x in FCC flue gas with a riser reactor.

Table 1
Major removals and reactions of flue gas purification with activated carbon (Olson et al., 2000).

Items	Explanation
Activated carbon adsorption	
Solid particles adsorbed by carbon	Removal of fine catalyst particulates
$O_2(g) = 2O(ad)$	Removal of O_2
$SO_2(g) + O(ad) + H_2O(ad) = H_2SO_4(ad)$	Removal of O_2
$SO_3(g) + H_2O(ad) = H_2SO_4(ad)$	Conversion of SO_3 to H_2SO_4
$H_2SO_4(ad) + 2NH_3(g) = (NH_4)_2SO_4(ad)$	Conversion of H_2SO_4 to $(NH_4)_2SO_4$
$NO(g) + O(ad) = NO_2(ad)$	Removal of NO and O_2
$2NO_2(ad) + 2NH_3(g) = 2N_2(g) + 3H_2O(g) + O(ad)$	Removal of NO_2
Activated carbon regeneration	
$(NH_4)_2SO_4(ad) = SO_3(ad) + H_2O(g) + 2NH_3(g)$	Degradation of $(NH_4)_2SO_4$ to SO_3
$NH_3(g) + 3SO_3(ad) = SO_2(g) + N_2(g) + H_2O(g)$	Reduction of SO_3 to SO_2

Note: (ad) = adsorbed state, (g) = gas phase.

diluted with N_2. These standard gases were purchased from Beijing Huatong Precision Chemical Gases Company. The FCC heavy oil feedstock, FCC fresh catalyst and FCC equilibrium catalyst were obtained from Sinopec Yanshan Petrochemical Company. The detailed properties of the two FCC catalysts are shown in Table 2. The properties of heavy oil feedstock are shown in Table 3.

2.2.2. Experimental procedure and product analysis

The aim of this study was to investigate the complete conversion of SO_x to H_2S in a riser reactor under the influence of a dry gas prelift. The prelift dry gas mainly contains H_2, methane (CH_4), and ethane (C_2H_6), which have relatively high H_2 contents. Therefore, low-concentration reducing gases (H_2 gas, CH_4 and C_2H_6 mix gas, and H_2, CH_4 and C_2H_6 mix gas) were selected as typical reactants to verify the feasibility of completely reducing SO_2 in the riser.

As depicted in Fig. 2, a small tube reactor (STR) is employed to simulate reduction reactions in the riser reactor. A mass flow controller (MFC) is utilized to determine the gas flow. The gas enters from the upper part of the reactor, which has an inner diameter of 16 mm. The tube reactor is heated in three distinct zones, with the middle zone serving as the catalyst loading zone. After the gas is cooled in the condenser, a portion of the gas is analyzed online by a sulfide content tester, while another portion is vented.

The typical experimental procedure follows: the reducing gas (6 v% H_2) is introduced into the reducing gas line, which is controlled by a gas mass flow meter. The SO_2 standard gas (1 v% SO_2) is introduced into the SO_2 gas line, which is also controlled by a gas mass flow meter. Both lines are connected to the upper part of the small tube reactor. The reaction is terminated by turning off the two gas mass flow meters. The postreaction gases are then cooled by a condenser, an ion chromatograph is used to analyze the water solution in condenser, and a GC 5890 gas chromatograph is used to analyze some of the gases. Five consecutive measurements are averaged with an error of less than 2%.

Table 2
The properties of the FCC catalysts.

Property	FCC fresh catalyst	FCC equilibrium catalyst
Pore volume, cm^3/g	0.32	0.28
Specific surface area, m^2/g	148	135
Micro-reactivity index	77	58
Chemical composition, wt%		
Al_2O_3	54.4	53.32
SiO_2	42.79	41.95
P_2O_5	2.24	2.20
MgO	0.22	0.22
ZnO	0.31	0.31
MnO	0.04	0.04
Fe_2O_3	0	0.59
NiO	0	0.98
V_2O_5	0	0.39

Table 3
The properties of heavy oil feedstock.

Items	Value	Items	Value
Feedstock density (20 °C), $g \cdot cm^{-3}$	0.8986	Aromatics	18.9
Residual carbon value, wt%	3.01	Resins	12.4
Elemental content, wt%		Asphaltenes	<0.1
C	86.12	Boiling range, °C	
H	13.15	Initial boiling point	302
S	0.35	10 wt%	420
N	0.36	30 wt%	475
Hydrocarbon group composition, wt%		50 wt%	515
Saturates	68.7	70 wt%	543

The definitions of SO_x conversion and H_2S selectivity in the experimental and thermodynamic computations are shown as follows:

$$SO_x \text{ Conversion} = \left(1 - \frac{M_{\text{unconverted SOx}}}{M_{\text{SOx in feed}}}\right) \times 100\% \quad (3)$$

$$H_2S \text{ Selectivity} = \frac{M_{\text{sulfur in } H_2S \text{ product}}}{M_{\text{sulfur in } SO_x \text{feed}}} \times 100\% \quad (4)$$

In order to examine the heavy oil FCC performance with FCC equilibrium catalyst before and after SO_2 reduction in detail. The heavy oil FCC experiments were carried out in a fixed fluidized bed reactor, the schematic diagram is shown in Fig. 3, and the experimental conditions were: Temperature was 550 °C, catalyst/oil mass ratio was 12, and weight hourly space velocity (WHSV) was 10 h^{-1}. Additional details of the operation of this device are given in the literature (Yang et al., 2023).

2.2.3. Product analysis

The SO_2 content in the exit gas samples at each experimental point was analyzed. While the simulation experiment aims to determine whether SO_2 is completely converted to H_2S, only the H_2S content in the exit gas samples is analyzed when the SO_2 conversion reaches 100%. A GC 5890 gas chromatograph with a flame photometric detector (FPD) was used to analyze various sulfide fractions (including H_2S, sulfur, and SO_2) in the exit gas samples from the small tube reactor. The chromatographic data were analyzed using an N(VI) 3000 chromatographic workstation. For the experimental points with 100 percent H_2S yield, the sulfate and sulfite of the water solution in condenser was analyzed using an ion chromatograph (ICS-1100, Thermo Dionex), the results show that these ions were not exist in the water, suggesting that SO_2 is completely converted to H_2S.

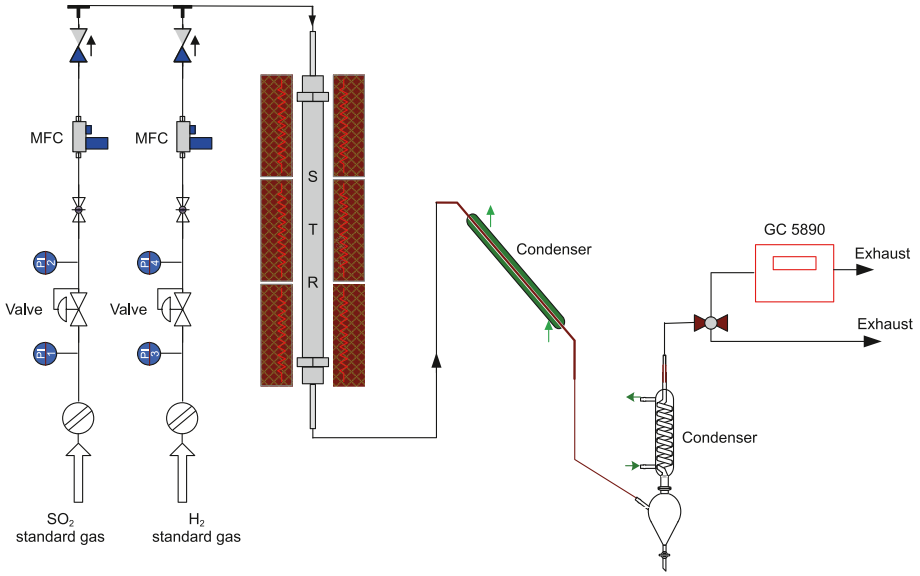


Fig. 2. Schematic diagram of experimental SO_2 reduction in a small tubular reactor.

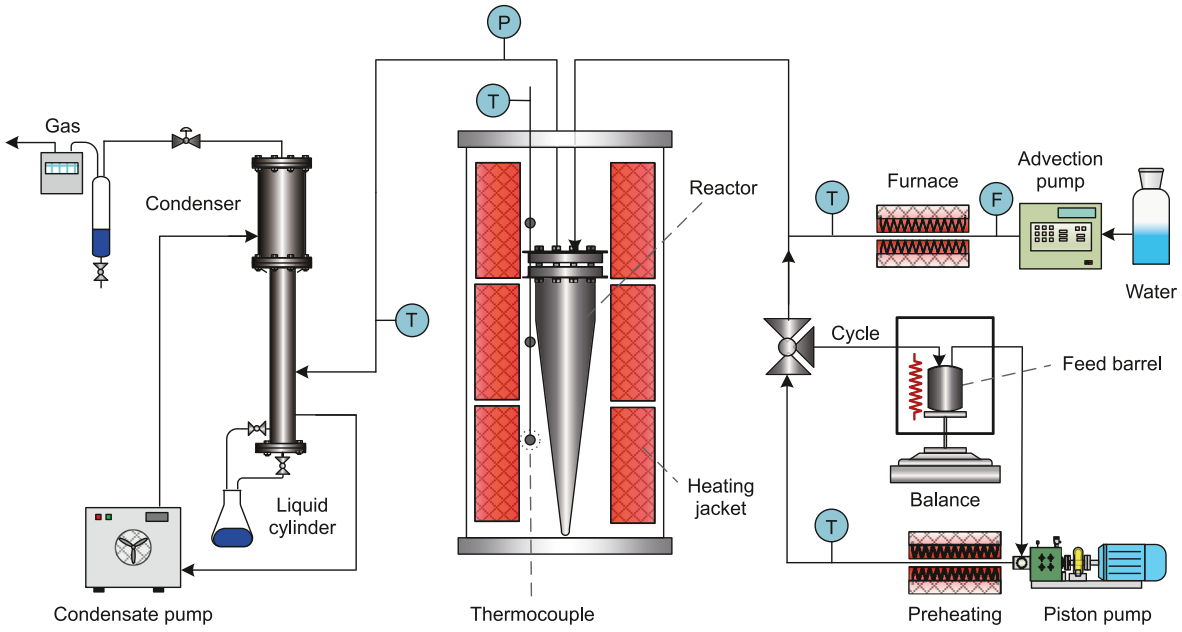


Fig. 3. Schematic diagram of fixed fluidized bed experimental reactor.

The FCC gas product was defined as cracked gas (H_2 and C_1–C_4 hydrocarbons). The hydrocarbon percentage of cracked gas was analyzed by Agilent 6890 chromatography, the sulfur content of cracked gas was obtained from GC 5890 gas chromatograph. The liquid product was classified into gasoline (C_5-200 °C), diesel (200–350 °C) and slurry oil (Initial boiling point >350 °C), and a small distillation setup was used to cut out gasoline, diesel and slurry oil, more details of this device are given in the previous literature (Wang, 2006). The sulfur content of gasoline, diesel and slurry oil were analyzed by an RPP200S UV Fluorescence Sulfur Analyser. The hydrocarbon composition of the gasoline was obtained by another Agilent 7890 chromatography. The coke and sulfur content on the catalyst was determined by an infrared carbon and sulfur analyzer.

The micro-activity of the catalyst was determined using a WFS-1D automatic micro inverse activity tester from Sinopec Research Institute of Petroleum Processing. The structural groups on the FCC equilibrium catalyst were detected using a Nicolet Magma-IR 560 ESP FTIR spectrometer manufactured in the USA. The Bruker D8 Advance equipment with Cu Kα radiation was used to test X-ray diffraction (XRD) patterns of catalysts. The specific surface area and pore volume of the catalysts were measured using a Quadrasorb-SI multifunctional adsorber manufactured in the USA, using high purity nitrogen as the adsorbent. The BET equation was used to determine the specific surface area, and the t-plot method was used to calculate the pore volume.

3. Results and discussion

3.1. Reaction system analysis for the reduction of SO_x in riser

The FCC-DeSO_x process revolves around the solid reduction environment in the riser and the action of the prelift dry gas (H_2-rich). Through process innovation, the efficient recovery and conversion of sulfur resources in FCC flue gas can be achieved, significantly increasing the treatment capacity of FCC flue gas. The reduction process of SO_x is divided into three reaction zones based on the relative concentration of reactants, temperature, and residence time in different zones of the riser. Please refer to Table 4 for the detailed conditions.

A schematic representation of a typical process flow for the reduction of SO_x in a riser reactor is presented in Fig. 4. SO_x gas, combined with prelift dry gas, enters the prelift reaction zone (reaction zone 1). In this zone, the mixed gas is brought into contact with the high-temperature FCC catalyst to facilitate a reduction reaction, resulting in the reduction of SO_x. Subsequently, the mixed gas, along with the high-temperature catalyst, move upward into the riser zone. In the lower zone (reaction zone 2) of the riser, petroleum hydrocarbons, mixed gas, and catalyst come into contact, leading to the formation of a mixture of materials. During this contact, the SO_x is primarily reduced through the FCC liquid phase products. The resulting mixture then enters the upper zone (reaction zone 3) of the riser, where further reduction of SO_x occurs through the FCC cracked gas. After undergoing reduction in these three reaction zones, the SO_x is fully reduced to H_2S.

The H_2S-rich FCC product is then guided through a fractional distillation tower, an absorption stabilization unit, and a dry gas refining device. These components collectively facilitate the production of H_2S with high purity and increase the availability of raw materials for the sulfur unit. Additionally, it is possible to feed SO_x into different zones within the riser reactor, ensuring complete conversion to H_2S after undergoing reduction reactions in reaction zones 1 to 3. If SO_x is only fed into reaction zone 3, the residence time is minimized, thereby reducing its impact on the FCC product.

Throughout the SO_x reduction process, the elemental sulfur in SO_x may be reduced directly by hydrocarbons into H_2S or sulfur, and SO_x or H_2S may also combine with hydrocarbon to form organic sulfides (mercaptans, thiophenes, benzothiophenes, and coke), therefore, in this paper, the thermodynamic theoretical calculations are examined for the reduction of SO_2 to form H_2S and the reaction to form organic sulfides. For the reduction of SO_2 by hydrocarbons to form H_2S or sulfur, a selection of compounds, including H_2, CH_4, C_2H_6, ethylene (C_2H_4), propane (C_3H_8), propylene (C_3H_6), 1-butene (n-C_4H_8), and n-butane (n-C_4H_{10}), were chosen to represent FCC cracked gas. Additionally, n-heptane (n-C_7H_{16}), 1-heptene (1-C_7H_{14}), methylcyclohexane (Cyc-C_7H_{14}), methylbenzene (C_7H_8) and Phenanthrene ($C_{14}H_{10}$) were chosen to represent FCC liquid products. Heptazethrene ($C_{28}H_{16}$) was chosen to represent polycyclic aromatic hydrocarbon (PAH) in FCC coke. For typical organic sulfides generated during the FCC process, heptanethiol ($C_7H_{16}S$), propylthiophene ($C_7H_{10}S$), 2,5-dimethylthiophene (C_6H_8S), benzothiophene (C_8H_6S) were chosen to represent sulfide in FCC liquid products, a sulfur-containing polycyclic aromatic hydrocarbon (S-PAH) $C_{28}H_{20}S$ was chosen to represent sulfide in FCC coke.

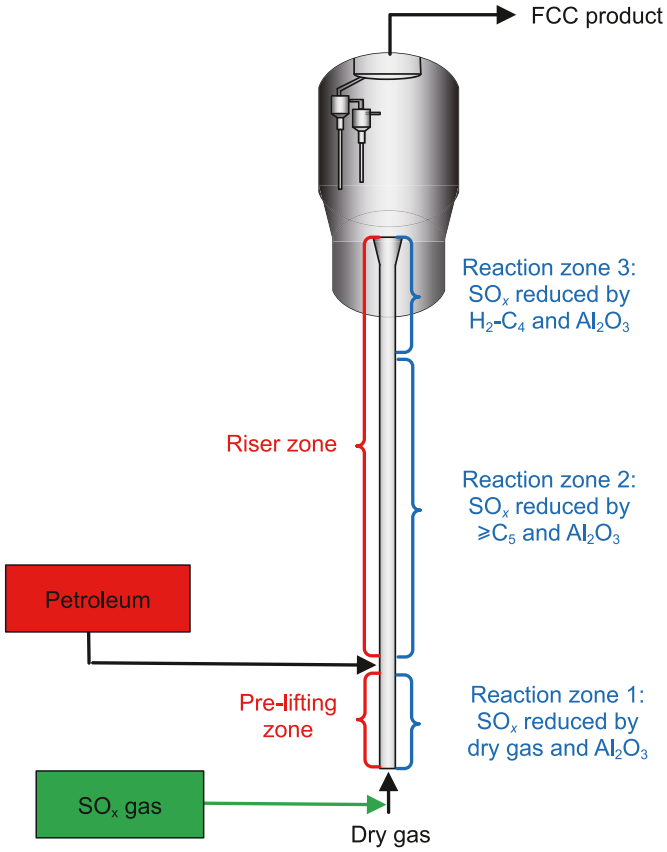


Fig. 4. Schematic diagram of the process for reducing SO_x in a riser apparatus.

It is important to note that under FCC conditions, the catalyst remains in a solid state, while all other reactants are gaseous. Furthermore, the molar ratio of SO_2 to SO_3 in SO_x is maintained at 100:1, and the reduction products of SO_x are either H_2S or S_2. To exemplify the reactions involved in reducing SO_2, Table 5 provides an overview of the central zones and typical reaction equations in the riser reactor. The main reactions associated with the catalyst are shown in reactions 1–7, including the reaction of alumina (the main component of the FCC catalyst) with SO_x to form sulfate or sulfite, and the reduction of sulfate or sulfite by hydrogen or hydrocarbons to sulfide salts, oxides, and similar byproducts. Since the catalysts are distributed throughout the reactor, these reactions are taken into account in all three reaction zones, for the prelift zone and the upper zone of the riser, the sulfate reduction is mainly H_2 in the H_2-rich cracked gas (n = 0 in the relative reaction equation), and for the lower zone of the riser, the sulfate reduction is mainly with the C_5–C_{12} hydrocarbons, n-heptane (n-C_7H_{16}) is chosen in this study.

Table 4
The reduction reaction zones of SO_x in the riser reactor.

Name	Reaction zone 1	Reaction zone 2	Reaction zone 3
Position	Pre-lift zone	Lower zone of the riser	Upper zone of the riser
Temperature, °C	600–650	500–600	450–550
Residence time, s	0–3	1–3	1–3
Main reactant	Prelift dry gas (H_2, CH_4, C_2H_6) and catalyst	FCC liquid products ($\geq C_5$ hydrocarbons) and catalyst	FCC cracked gas (H_2 and C_1–C_4 hydrocarbons) and catalyst

Table 5
Summary of main SO_x-reduced reactions in riser reactor.

Number	Reaction equations	Reaction zone
1	$Al_2O_3(s) + 3SO_3 = Al_2(SO_4)_3(s)$	1–3
2	$Al_2O_3(s) + 3SO_2 = Al_2(SO_3)_3(s)$	1–3
3	$Al_2(SO_4)_3(s) + 12C_nH_{2n+2} = Al_2S_3(s) + 12H_2O + 12C_nH_{2n}$	1–3
4	$Al_2(SO_4)_3(s) + 12\ C_nH_{2n+2} = Al_2O_3(s) + 9H_2O + 3H_2S + 12C_nH_{2n}$	1–3
5	$Al_2(SO_3)_3(s) + 9\ C_nH_{2n+2} = Al_2S_3(s) + 9H_2O + 9C_nH_{2n}$	1–3
6	$Al_2(SO_3)_3(s) + 9\ C_nH_{2n+2} = Al_2O_3(s) + 6H_2O + 3H_2S + 9C_nH_{2n}$	1–3
7	$Al_2S_3(s) + 3H_2O = Al_2O_3(s) + 3H_2S$	1–3
8	$3H_2 + SO_2 = H_2S + 2H_2O$	1
9	$3/4CH_4 + SO_2 = H_2S + 1/2H_2O + 3/4CO_2$	1
10	$3/7C_2H_6 + SO_2 = H_2S + 2/7H_2O + 6/7CO_2$	1
11	$2H_2 + SO_2 = 1/2S_2 + 2H_2O$	1
12	$1/2CH_4 + SO_2 = 1/2S_2 + H_2O + 1/2CO_2$	1
13	$2/7C_2H_6 + SO_2 = 1/2S_2 + 6/7H_2O + 4/7CO_2$	1
14	$3n\text{-}C_7H_{16} + SO_2 = H_2S + 31\text{-}C_7H_{14} + 2H_2O$	2
15	$3n\text{-}C_7H_{16} + SO_2 = H_2S + 3C_4H_8 + 3C_3H_6 + 2H_2O$	2
16	$1\text{-}C_7H_{14} + SO_2 = H_2S + C_7H_8 + 2H_2O$	2
17	$Cyc\text{-}C_7H_{14} + SO_2 = H2S + C_7H_8 + 2H_2O$	2
18	$2C_7H_8 + SO_2 = H_2S + C_{14}H_{10} + 2H_2O$	2
19	$0.5C_7H_8 + 0.51\text{-}C_7H_{14} + SO_2 = H_2S + 0.5C_{14}H_{10} + 2H_2O$	2
20	$3C_{14}H_{10} + SO_2 = H_2S + 2H_2O + 1.5C_{28}H_{18}$	2
21	$2n\text{-}C_7H_{16} + SO_2 = 1/2S_2 + 21\text{-}C_7H_{14} + 2H_2O$	2
22	$2n\text{-}C_7H_{16} + SO_2 = 1/2S_2 + 2C_4H_8 + 2C_3H_6 + 2H_2O$	2
23	$2/31\text{-}C_7H_{14} + SO_2 = 1/2S_2 + 2/3C_7H_8 + 2H_2O$	2
24	$2/3\ Cyc\text{-}C_7H_{14} + SO_2 = 1/2S_2 + 2/3C_7H_8 + 2H_2O$	2
25	$4/3C_7H_8 + SO_2 = 1/2S_2 + 2/3C_{14}H_{10} + 2H_2O$	2
26	$1/3C_7H_8 + 1/31\text{-}C_7H_{14} + SO_2 = 1/2S_2 + 1/3C_{14}H_{10} + 2H_2O$	2
27	$4C_{14}H_{10} + SO_2 = 1/2S_2 + 2H_2O + 2C_{28}H_{18}$	2
28	$1\text{-}C_6H_{12} + SO_2 = C_6H_8S + 2H_2O$	2
29	$1\text{-}C_7H_{14} + SO_2 = C_7H_{10}S + 2H_2O$	2
30	$1/2\ 1\text{-}C_8H_{16} + SO_2 = 1/2C_8H_6S + 1/2H_2S + 2H_2O$	2
31	$3/10C_{14}H_{10} + SO_2 + 3/5C_7H_{14} = 2H_2O + 7/10H_2S + 3/10C_{28}H_{20}S$	2
32	$1\text{-}C_7H_{14} + H_2S = C_7H_{16}S$	2
33	$19/10C_{14}H_{10} + H_2S + 1/51\text{-}C_7H_{14} = C_{28}H_{20}S + 19/10H_2$	2
34	$C_7H_{14} + H_2S = C_7H_{10}S + 3H_2$	2
35	$1\text{-}C_8H_{16} + H_2S = C_8H_6S + 6H_2$	2
36	$3H_2 + SO_2 = H_2S + 2H_2O$	3
37	$3/4CH_4 + SO_2 = H_2S + 1/2H_2O + 3/4CO_2$	3
38	$3/7C_2H_6 + SO_2 = H_2S + 2/7H_2O + 6/7CO_2$	3
39	$1/2C_2H_4 + SO_2 = H_2S + CO_2$	3
40	$3/10C_3H_8 + SO_2 = H_2S + 9/10CO_2 + 1/5H_2O$	3
41	$1/3C_3H_6 + SO_2 = H_2S + CO_2$	3
42	$3/13n\text{-}C_4H_{10} + SO_2 = H_2S + 12/13CO_2 + 2/13H_2O$	3
43	$1/4n\text{-}C_4H_8 + SO_2 = H_2S + CO_2$	3
44	$2H_2 + SO_2 = 1/2S_2 + 2H_2O$	3
45	$1/2CH_4 + SO_2 = 1/2S_2 + H_2O + 1/2CO_2$	3
46	$2/7C_2H_6 + SO_2 = 1/2S_2 + 6/7H_2O + 4/7CO_2$	3
47	$1/3C_2H_4 + SO_2 = 1/2S_2 + 2/3CO_2 + 2/3H_2O$	3
48	$1/5C_3H_8 + SO_2 = 1/2S_2 + 3/5CO_2 + 4/5H_2O$	3
49	$2/9C_3H_6 + SO_2 = 1/2S_2 + 2/3CO_2 + 2/3H_2O$	3
50	$2/13n\text{-}C_4H_{10} + SO_2 = 1/2S_2 + 8/13CO_2 + 10/13H_2O$	3
51	$1/6n\text{-}C_4H_8 + SO_2 = 1/2S_2 + 2/3CO_2 + 2/3H_2O$	3

For the reduction of SO_x by H_2 or hydrocarbons, the prelift zone includes reactions 8–13, involving the H_2, CH_4 and C_2H_6 reduction of SO_x to H_2S or S_2. Reactions 14–35, taking place in the lower zone of the riser, reactions 14–27 show the reduction of SO_2 by FCC liquid products, primarily alkanes undergoing direct dehydrogenation or cracking dehydrogenation, olefins undergoing cyclization and aromatization dehydrogenation, cycloalkanes being dehydrogenated, and aromatics participating in condensation with olefins or other aromatics to facilitate dehydrogenation. Reactions 28–31 depict the formation of thiophene and benzothiophene compounds from olefins and SO_2, and the generation of S-PAH from aromatics, olefins and SO_2. In the upper zone of the riser, reactions 36–51 involve the reduction of SO_2 by FCC cracked gas, resulting in the generation of CO_2, H_2S, or S_2 as the primary products.

3.2. Thermodynamic analysis of SO_x reduction in riser

3.2.1. Thermodynamic equilibrium of the reactions

Upon entering the riser, SO_x undergoes a reduction in the 1–3 reaction zones. This study calculates the Gibbs free energy (ΔG) and thermodynamic constants (k) for typical reactions 1–51 based on the information presented in Table 5. The variations in $-\Delta G$ and log k with reaction temperature for different reactions are illustrated in Fig. 5(a)–5(h). Notably, the log k values for all reduction reactions, except for the dehydrogenation of alkanes to reduce SO_2 to S_2, exceeded 5. This suggests that when thermodynamic equilibrium is achieved, SO_2 can be completely reduced. Moreover, when the reduction product is H_2S, the values of $-\Delta G$ and log k are more pronounced than when the product is S_2, sulfur-containing salts, thiophene or S-PAH. Consequently, it becomes more difficult for S_2, sulfur-containing salts, thiophene or S-PAH to form, and SO_2 is thermodynamically more inclined to be reduced to H_2S in the 3

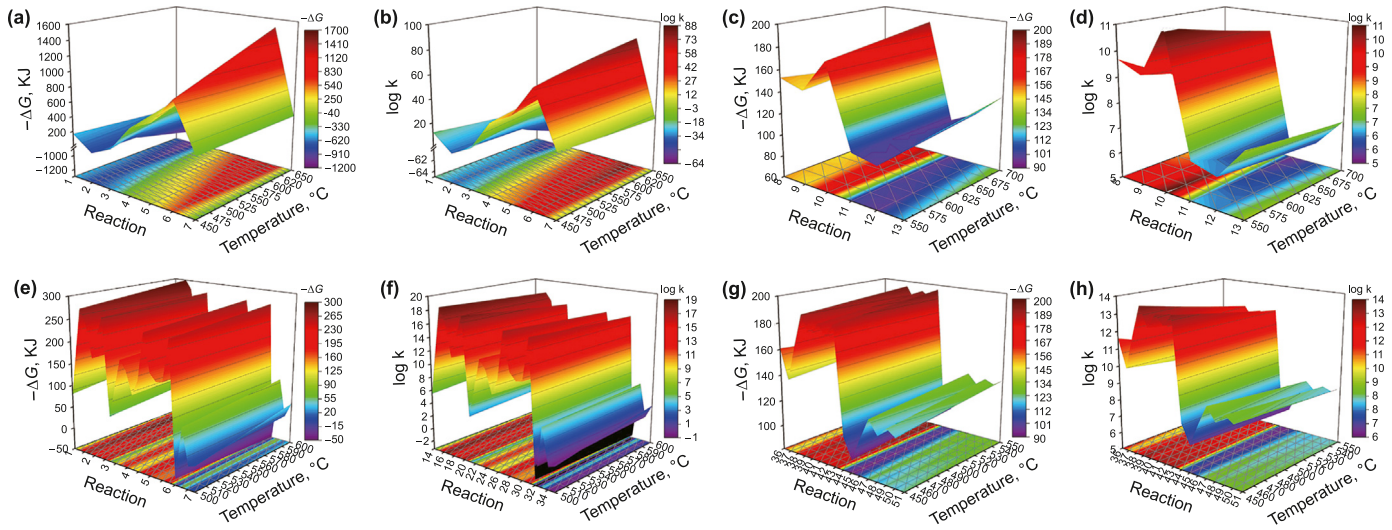


Fig. 5. Schematic diagram of $-\Delta G$ and log k of reduction of SO_x in riser reactor. **(a)** $-\Delta G$ for catalyst-related reactions in the three reaction zones, **(b)** log *k* for catalyst-related reactions in the three reaction zones, **(c)** $-\Delta G$ in dry gas (H_2-rich) pre-lift zone, **(d)** log *k* in dry gas (H_2-rich) pre-lift zone, **(e)** $-\Delta G$ in the lower zone of riser, **(f)** log *k* in the lower zone of riser, **(g)** $-\Delta G$ in the upper zone of riser, **(h)** log *k* in the upper zone of riser.

reaction zones. For the reactions of H_2S with olefins and aromatics to form sulfur-containing hydrocarbons, the formation of thiols or thiophenes' log *k* is less than 3, the log *k* of the sulfur-containing coke formation exceeds 5. Considering the susceptibility of thiophenes to condensation to form S-PAH, H_2S is thermodynamically likely to increase the sulfur content of coke.

As depicted in Fig. 5(a)–5(b), in the three reaction zones (450–650 °C), the log *k* for the generation of sulfate or sulfite significantly decreases as the temperature increases. On the other hand, the log *k* for the generation of aluminum sulfide from the hydrogen or hydrocarbons reduction of alumina sulfate increases, while the log *k* for other reduced sulfur-containing species only slightly decreases. These observations indicate that higher reaction temperatures are favorable for the conversion of SO_x to H_2S in the

Table 6
Typical FCC conditions and product distribution of heavy oil in riser.

Items	Value	Items	Value
Feedstock density (20 °C), g·cm^{-3}	0.8986	Gasoline composition, wt%	
Sulfur content, wt%	0.35	Paraffin	27.27
Temperature, °C		Olefin	34.56
Pre-lift zone, °C	660	Naphthene	6.90
Lower zone of the riser, °C	570	Aromatics	31.27
Upper zone of the riser, °C	550	Cracked gas composition, wt%	
Residence time, s	1.24	Hydrogen (H_2)	1.61
Mass ratio of catalyst to oil	15	Methane (CH_4)	3.71
Distribution of products, wt%		Ethane (C_2H_6)	2.39
Cracked gas (H_2-C_4)	22.57	Ethylene (C_2H_4)	5.81
Gasoline (C_5-200 °C)	39.63	Propane (C_3H_8)	3.57
Diesel (200–350 °C)	18.64	Propylene (C_3H_6)	30.39
Slurry oil (>350 °C)	11.66	Butanes (C_4H_{10})	16.2
Coke	7.49	Butenes (C_4H_8)	36.32

Table 7
The molar quantity of initial reducing reactants in the riser reactor.

Name	Molar quantity	Name	Molar quantity
SO_x gas		C_7H_8	0.249
SO_2	1.000	Al_2O_3	43.000
SO_3	0.010	Upper zone of the riser	
Pre-lift zone		H_2	3.000
H_2	3.000	CH_4	0.865
CH_4	0.865	C_2H_6	0.297
C_2H_6	0.297	C_2H_4	0.775
Al_2O_3	43.000	C_3H_8	0.303
Lower zone of the riser		C_3H_6	2.702
C_7H_{16}	0.200	C_4H_{10}	1.043
1-C_7H_{14}	0.259	C_4H_8	2.422
Cyc-C_7H_8	0.052	Al_2O_3	43.000

Note: The molar quantity of SO_2 in the table are baseline 1 mol, and other species are based on SO_2.

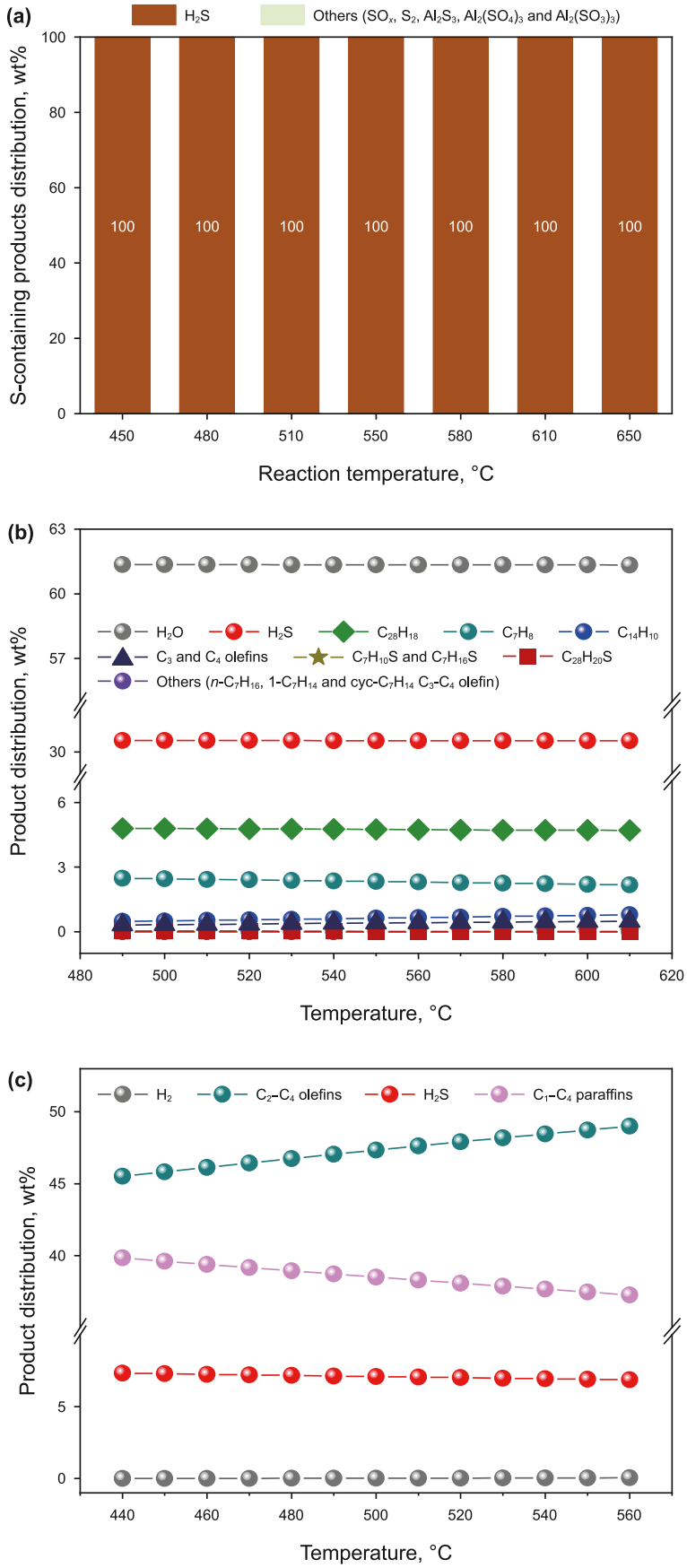


Fig. 6. Products distribution after SO_x reduction in riser after thermodynamic equilibrium. **(a)** Equilibrium distribution of sulfur-containing products in dry gas (H_2-rich) pre-lift zone, **(b)** Equilibrium distribution of products in the lower zone of riser, **(c)** Equilibrium distribution of products in the upper zone of riser.

Table 8
The initial molar ratio of reactants in the experiment.

Item	Value	Item	Value
SO_2 reduced by H_2		SO_2 reduced by H_2, CH_4 and C_2H_6	
Initial H_2/SO_2, mol/mol	8:1	Initial H_2/SO_2, mol/mol	8:1
SO_2 reduced by CH_4 and C_2H_6		Initial CH_4/SO_2, mol/mol	9:1
Initial CH_4/SO_2, mol/mol	9:1	Initial C_2H_6/SO_2, mol/mol	3:1
Initial C_2H_6/SO_2, mol/mol	3:1	/	/

riser.

By comparing the magnitudes of $-\Delta G$ and log k for SO_2 reduction of different hydrocarbons in the prelift, lower and upper zones of the riser (450–650 °C), as shown in Fig. 5(c)–5(h), we can obtain the following information: hydrocarbon aromatization, condensation dehydrogenation, and cleavage dehydrogenation for SO_2 reduction are strong, suggesting that SO_2 is more likely to be reduced by hydrogen during these reactions, during the aromatic condensation process, the combination of aromatics with SO_2 to form S-PAH is also significant. Consequently, elemental S is more prone to form coke or cracked gas when thermodynamic equilibrium is reached. Compared with alkanes, olefins possess a greater ability to reduce SO_2. Therefore, the content of olefins in FCC cracked gas may decrease after SO_2 passes into the upper zone of the riser. Furthermore, after the reaction reaches thermodynamic equilibrium, higher temperatures and a greater number of hydrocarbon carbons favor the reduction of SO_2.

3.2.2. Calculation of thermodynamic equilibrium concentration

To further investigate the thermodynamic equilibrium concentration of the reduction system, a pre-evaluation was first performed, as shown in Table 6 (Wang, 2006), the heavy oil feedstock sulfur content is 0.35 wt%, even if all the S in feedstock enters the FCC flue gas, the SO_x entering the riser is theoretically at most 0.9 wt% of the heavy oil mass, at this point, the molar ratio of FCC product H_2 to SO_x has exceeded 16. In the SO_x reduction process, we can increase the SO_x concentration by improving the SO_x flow. In the SO_x reduction thermodynamic equilibrium calculations, we set the reduced SO_x concentration larger than the theoretical value 16 to enhance the persuasiveness of the process in dealing with larger SO_x concentrations.

We made the following assumptions. First, we set the SO_2/SO_3 molar ratio in the SO_x gas to 100 in all three reaction zones. Second, considering that at least 3 mol of H_2 are required for the complete reduction of 1 mol of SO_2 to H_2S, we set the H_2/SO_2 molar ratio to 3 in the prelift zone and the upper zone of the riser, and set the C_7H_{16}/SO_2 molar ratio in the lower zone of the riser to 0.2. Then, for the prelift zone, as shown in Table 6 and if all H_2 is derived from the FCC product, the yield is approximately 0.36 wt%. With a catalyst-oil ratio of 15 and an Al_2O_3 content of approximately 50%, the Al_2O_3/H_2 molar ratio was 41. Finally, for the two reaction zones of the riser, the molar amounts of other reductants were calculated based on the composition of cracked gas and gasoline data from a typical FCC product distribution, as presented in Table 6. The calculated molar amounts of the initial reactants are displayed in Table 7.

The thermodynamic equilibrium compositions at different temperatures in the three reaction zones are illustrated in Fig. 6. Fig. 6(a)–6(c) indicates that Al_2S_3, $Al_2(SO_4)_3$, and $Al_2(SO_3)_3$ are not produced after reaching thermodynamic equilibrium. This signifies that the catalyst remains unaffected during the reduction of SO_x in the riser. Once thermodynamic equilibrium is reached, SO_x can be fully converted to H_2S at prelift zone and upper zone of the riser, H_2S selectivity exceeded 99.98% and sulfur-containing aromatics selectivity was less than 0.02% in the lower zone of the riser. This implies that SO_x is almost completely converted to H_2S in all three reaction zones of the reactor, only traces of S-PAHs are generated in the lower zone of the riser.

As shown in Fig. 6(b), after attaining thermodynamic equilibrium, the hydrocarbon products primarily consisted of $C_{28}H_{18}$, C_7H_8, $C_{14}H_{10}$ and C_3–C_4 olefins, S-containing products were mainly H_2S (about 30.5 wt%), with traces of S-PAH generated (0.01–0.03 wt %). This suggests that the reduction of SO_x by the FCC liquid products is mainly achieved through condensation dehydrogenation, aromatization dehydrogenation, and cracking dehydrogenation. As demonstrated in Fig. 6(b)–6(c), the reaction temperature decreases with the height of the riser, resulting in a gradual decrease in C_2–C_4 olefins and a gradual increase in C_1–C_4 alkanes, toluene and polycyclic aromatics. This implies that alkane cracking dehydrogenation reactions and the reduction of SO_x with C_1–C_4 alkanes are hindered, while the reduction of SO_x with C_2–C_4 olefins, the aromatization reaction to produce toluene and the aromatics condensation reaction are promoted. From a thermodynamic perspective, the consumption of olefins in the cracked gas may occur as the reaction temperature decreases or the residence time of SO_x increases. Moreover, SO_x reduction may result in slightly higher yield and sulfur content in coke.

3.3. Simulation of hydrogen reduction of SO_2 in riser

3.3.1. Preliminary experimental investigations

Thermodynamic equilibrium concentration calculations indicate that SO_x gas can be completely transformed into H_2S when introduced into the prelift zone, lower zone, and upper zone of the riser. Consequently, the primary objective in the industrial process of achieving complete reduction of SO_x to H_2S involves increasing the reaction rate or prolonging the reaction time to ensure that the reaction reaches thermodynamic equilibrium as quickly as possible. This can be accomplished by elevating the reaction temperature and employing catalysts to increase the reaction rate. In this study, an STR was utilized to simulate the riser reactor, for reducing SO_2 using H_2 gas, CH_4 and C_2H_6 mixed gas, H_2, CH_4 and C_2H_6 mixed gas, respectively. The initial reactants' molar ratio is shown in Table 8. Fig. 7 illustrates the conversion of the simulated reduction of SO_2.

In these experimental sets, when the SO_2 conversion reached 100%, H_2S selectivity was 100%. As depicted in Fig. 7(a), it is evident that the conditions required for complete conversion of SO_2 to H_2S are a reaction time of 5.4 s and a temperature above 600 °C when no FCC catalyst is utilized. The conversion of SO_2 to H_2S can be achieved by H_2 in the dry gas (H_2-rich) prelift zone (600–650 °C, 2.7 s, FCC fresh or equilibrium catalyst) and the riser zone (>475 °C, 2.7 s, FCC equilibrium catalyst). In the presence of FCC fresh catalyst, SO_2 can be entirely converted to H_2S when the reaction temperature exceeds 550 °C. Similarly, with the FCC equilibrium catalyst, SO_2 can be completely converted to H_2S at a reaction temperature above 475 °C.

By comparing the minimum reaction temperature required for the complete conversion of SO_2 to H_2S, it is observed that the FCC equilibrium catalyst requires a temperature 75 °C lower than that of the FCC fresh catalyst. This discrepancy can be attributed to the fact that the FCC equilibrium catalyst may contain higher

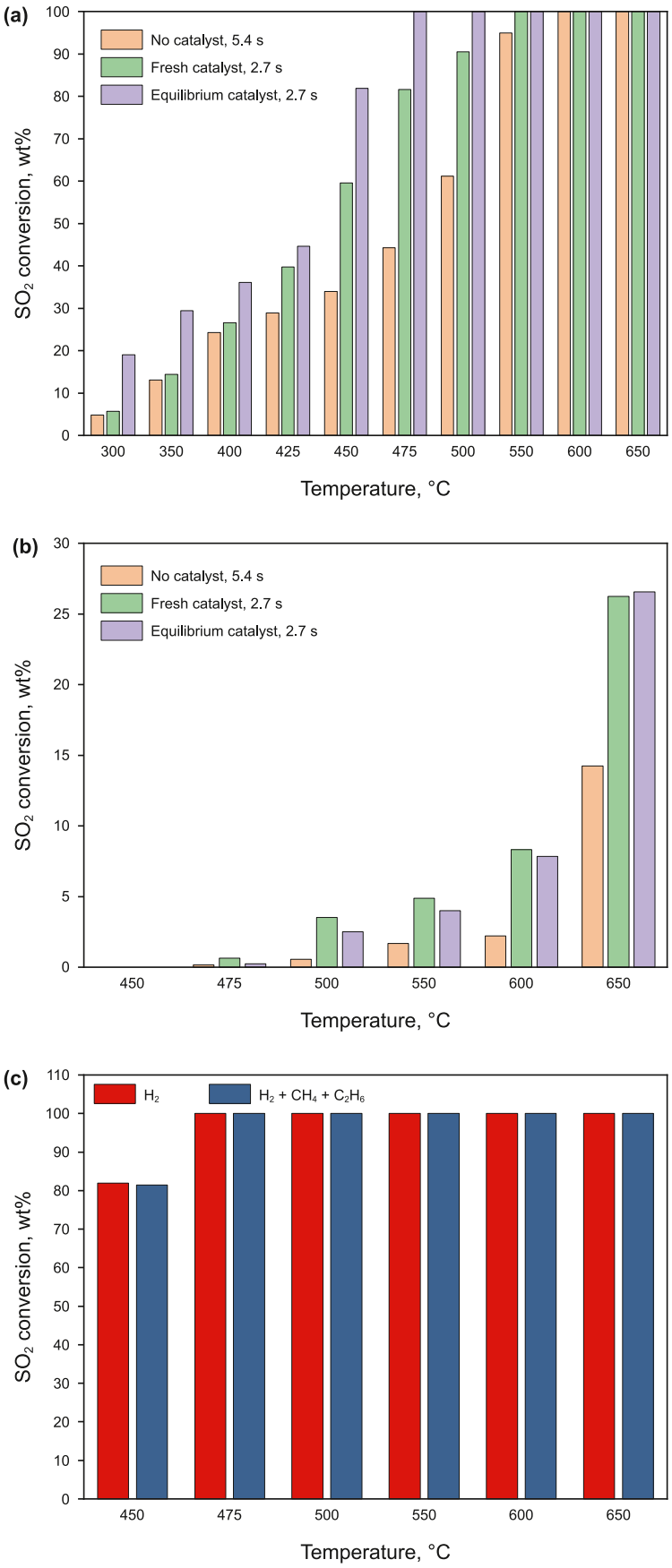


Fig. 7. SO_2 conversion under different reaction conditions. **(a)** SO_2 is reduced by hydrogen, **(b)** SO_2 is reduced by methane and ethane, **(c)** SO_2 is reduced by hydrogen or hydrogen, methane and ethane mixed gas with FCC equilibrium catalyst in 2.7 s.

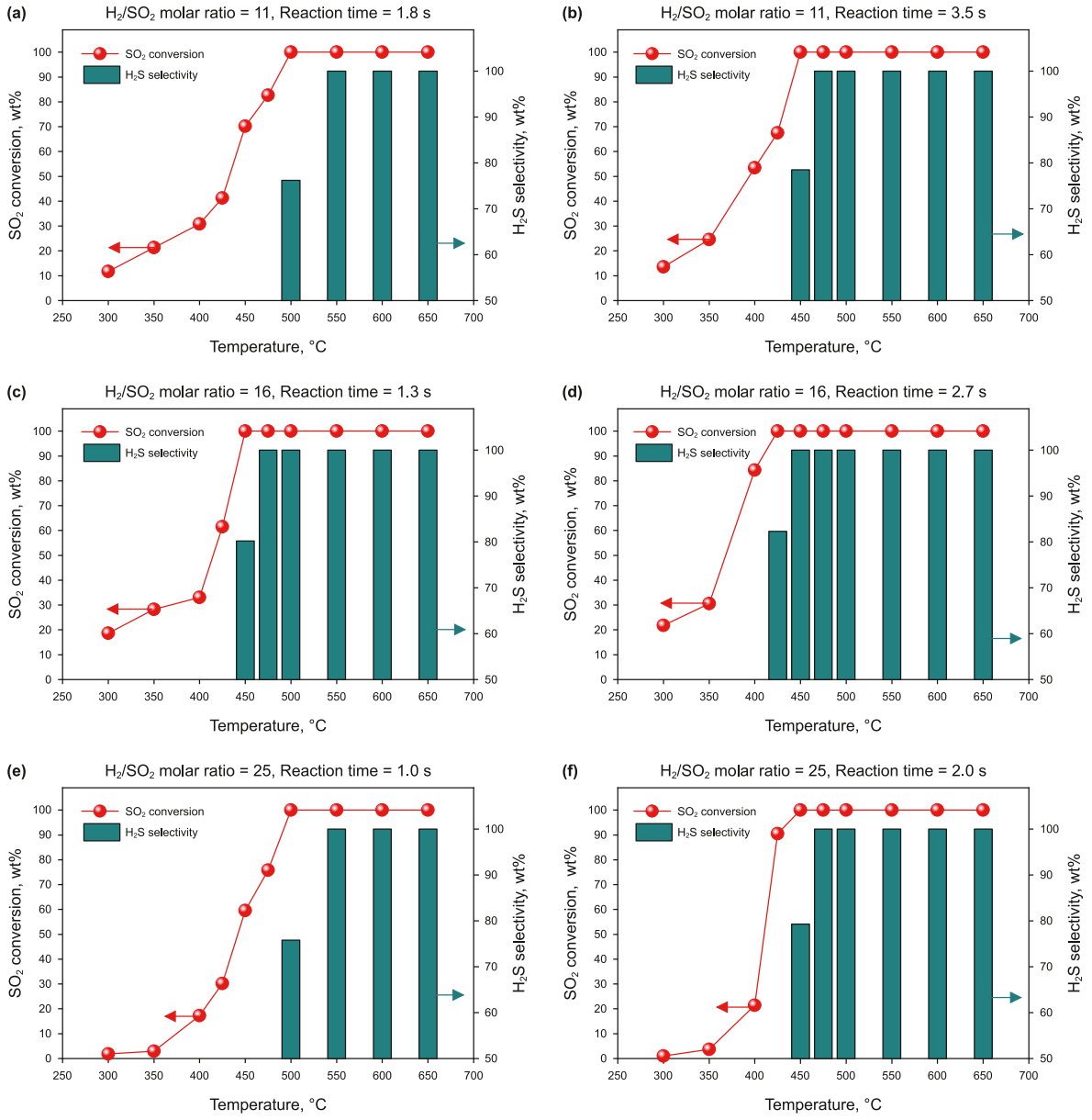


Fig. 8. SO_2 conversion and H_2S selectivity at different conditions. **(a)** H_2/SO_2 molar ratio = 11, reaction time = 1.8 s, **(b)** H_2/SO_2 molar ratio = 11, reaction time = 3.5 s, **(c)** H_2/SO_2 molar ratio = 16, reaction time = 1.3 s, **(d)** H_2/SO_2 molar ratio = 16, reaction time = 2.7 s, **(e)** H_2/SO_2 molar ratio = 25, reaction time = 1.0 s, **(f)** H_2/SO_2 molar ratio = 25, reaction time = 2.0 s.

concentrations of Fe, Ni, and V, some studies have shown that, these metals on the catalyst can promote the dissociation of hydrogen and facilitate the reduction of SO_2 (Doumani et al., 1944; Hu et al., 2002; Li and Hung, 2003; Wang et al., 2019). Consequently, the FCC equilibrium catalyst exhibits superior hydrogenation performance and is more conducive to the H_2 reduction of SO_2.

As shown in Fig. 7(b), the CH_4 and C_2H_6 mixed gas was used to reduce SO_2, and the SO_2 conversion below 30% all along, they are less efficient than H_2 in the SO_2 reduction. Fig. 7(c) further compares the reduction of SO_2 by H_2 or a mixture of H_2, CH_4 and C_2H_6, there is no difference in the SO_2 conversion, or H_2S yield between the two gases at the same temperature. It proves that SO_2 can be completely reduced to H_2S with dry gas (H_2, CH_4 and C_2H_6 mixed gas) above 475 °C. However, the introduction of CH_4 and C_2H_6 has no improvement on the SO_2 conversion and H_2S yield, and H_2 in the dry gas plays a primary role in the SO_2 reduction. Thus, the following study will focus on the reaction pattern of H_2 reduction of SO_2 under FCC conditions.

3.3.2. *Effect of conditions on the reduction of SO_2 by H_2*

The preceding results demonstrate that the reduction of SO_2 in the riser is influenced by both the kinetic reaction rate and the reaction time. The conversion of SO_2 can be controlled by adjusting the reaction temperature, H_2/SO_2 molar ratio, and reaction time. Notably, the reaction temperature has a significant impact on the reaction rate. The influence of the H_2/SO_2 molar ratio is more intricate. When the amount of SO_2 in the riser is held constant and the H_2/SO_2 molar ratio is increased, the corresponding reaction time decreases, thereby enhancing the contact between H_2 and SO_2 within a given timeframe. However, reducing the reaction time does not favor an increase in the conversion. To investigate the conversion behavior of SO_2 under different conditions, the

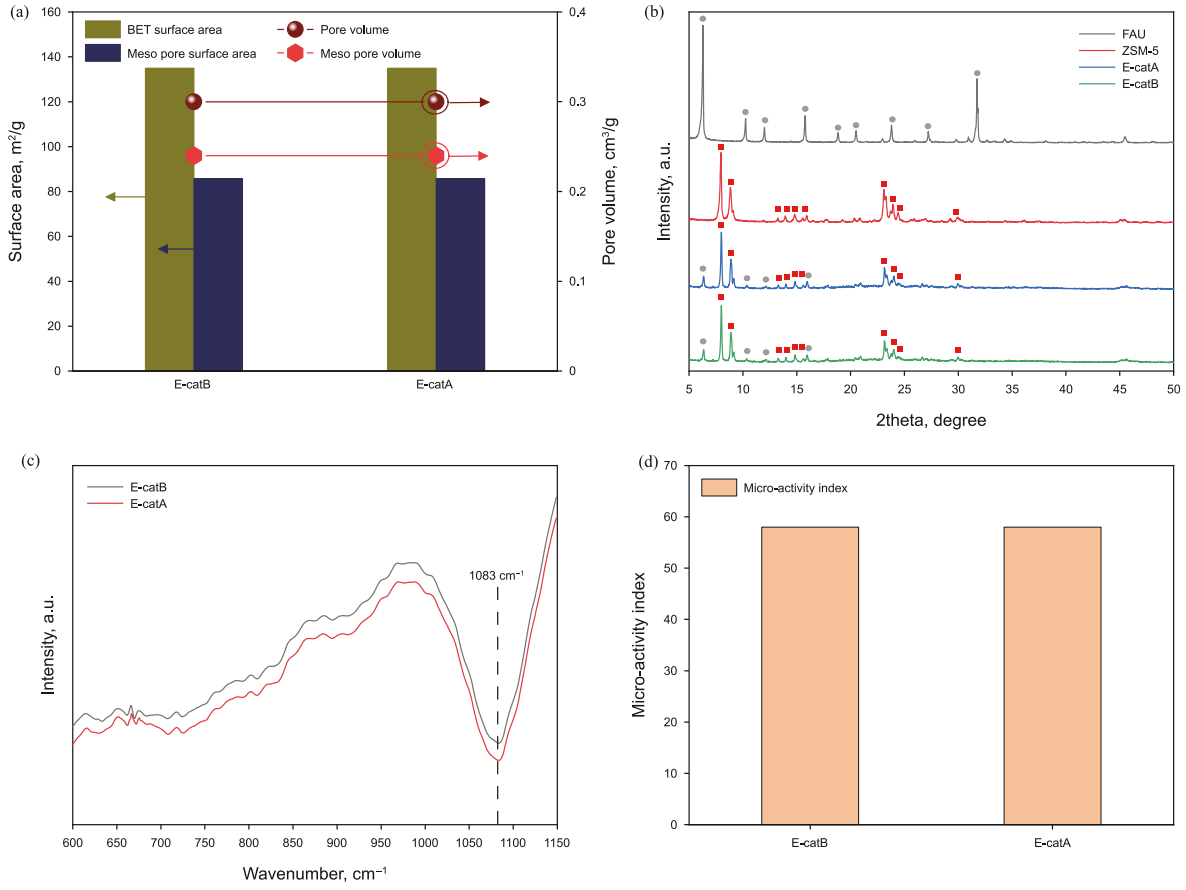


Fig. 9. Comparison of partial catalyst properties before and after SO_2 reduction. **(a)** Surface area and Pore volume, **(b)** XRD pattern, **(c)** FTIR spectra, **(d)** Micro-activity index.

influence of the H_2/SO_2 molar ratio and reaction time on SO_2 conversion and H_2S selectivity was examined at different reaction temperatures using an FCC equilibrium catalyst.

There are three main successive parallel reactions involved in the reduction of SO_2 by H_2: SO_2 reacts with H_2 to form H_2S, SO_2 reacts with H_2S to form sulfur, and sulfur is further reduced to H_2S by H_2 (Larraz, 2002). As illustrated in Fig. 8, prolonging the reaction time by 1–1.7 s decreases the minimum temperature required for the complete reduction of SO_2 to H_2S by 25–75 °C when the H_2/SO_2 molar ratio remains constant. This extension of the reaction time promotes the complete conversion of both SO_2 and sulfur into H_2S. Furthermore, it is noteworthy that the minimum temperature for the complete conversion of SO_2 to H_2S is slightly higher than the temperature for the complete conversion of SO_2 alone, indicating that higher reaction temperatures are favorable for enhancing H_2S selectivity.

By increasing the H_2/SO_2 molar ratio from 11 to 25, the reaction time for SO_2 reduction decreased from 1.8–3.5 s to 1–2 s. The reduction effect of SO_2 initially increases and then decreases, suggesting that the optimal conversion of SO_2 can be achieved by matching the appropriate H_2/SO_2 molar ratio and reaction time. In this case, the optimal molar ratio was 16, the reaction time was 1.3–2.7 s, and the temperature for the complete conversion of SO_2 to H_2S ranged from 450 to 475 °C.

3.3.3. Catalyst evaluation

FCC equilibrium catalyst before (E-catB) and after SO_2 reduction(E-catA) were characterized. E-catA was the post-SO_2 reduction (the H_2/SO_2 was 16 and H_2S yield was 100%) FCC equilibrium catalyst, and SO_2 reduction experiments were performed continuously for 5 h before characterisation. As shown in Fig. 9(c), the infrared absorption peak at 1083 cm^{-1} was attributed to the bidentate sulfate O=S=O covalent group (SO_4^{2-}) (Abdulhamid et al., 2006; Chen et al., 2011; Li et al., 2021), indicating that the equilibrium catalyst contains sulfate. As depicted in Fig. 9, the surface area, pore volume, XRD pattern, infrared spectra and microactivity of the FCC equilibrium catalyst remain unchanged before and after the SO_2 reduction. It demonstrated that no new group structures were produced on the catalyst after the SO_2 reduction.

Further examining the heavy oil FCC performance with E-catB and E-catA in detail. As depicted in Fig. 10, the product distributions, cracked gas composition, gasoline PONA composition, and product sulfur content were the same with two catalysts, indicating that the FCC equilibrium catalysts' catalytic cracking performance was unchanged after SO_2 reduction.

3.4. Lower limit of reaction time and kinetic modeling

3.4.1. Lower reaction time limit

During the reduction of SO_2, it is essential to minimize the reaction time in the riser to minimize its effect on the FCC reactions of petroleum hydrocarbons. To achieve this, the shortest reaction time for the complete reduction of SO_2 to H_2S by H_2 was investigated. The SO_2 conversion was examined at reaction times ranging from 0.1 to 0.7 s while maintaining a H_2/SO_2 molar ratio of 16. Additionally, the H_2S selectivity was evaluated when the SO_2 conversion reached 100%.

As depicted in Fig. 11(a), at a temperature of 600 °C and a

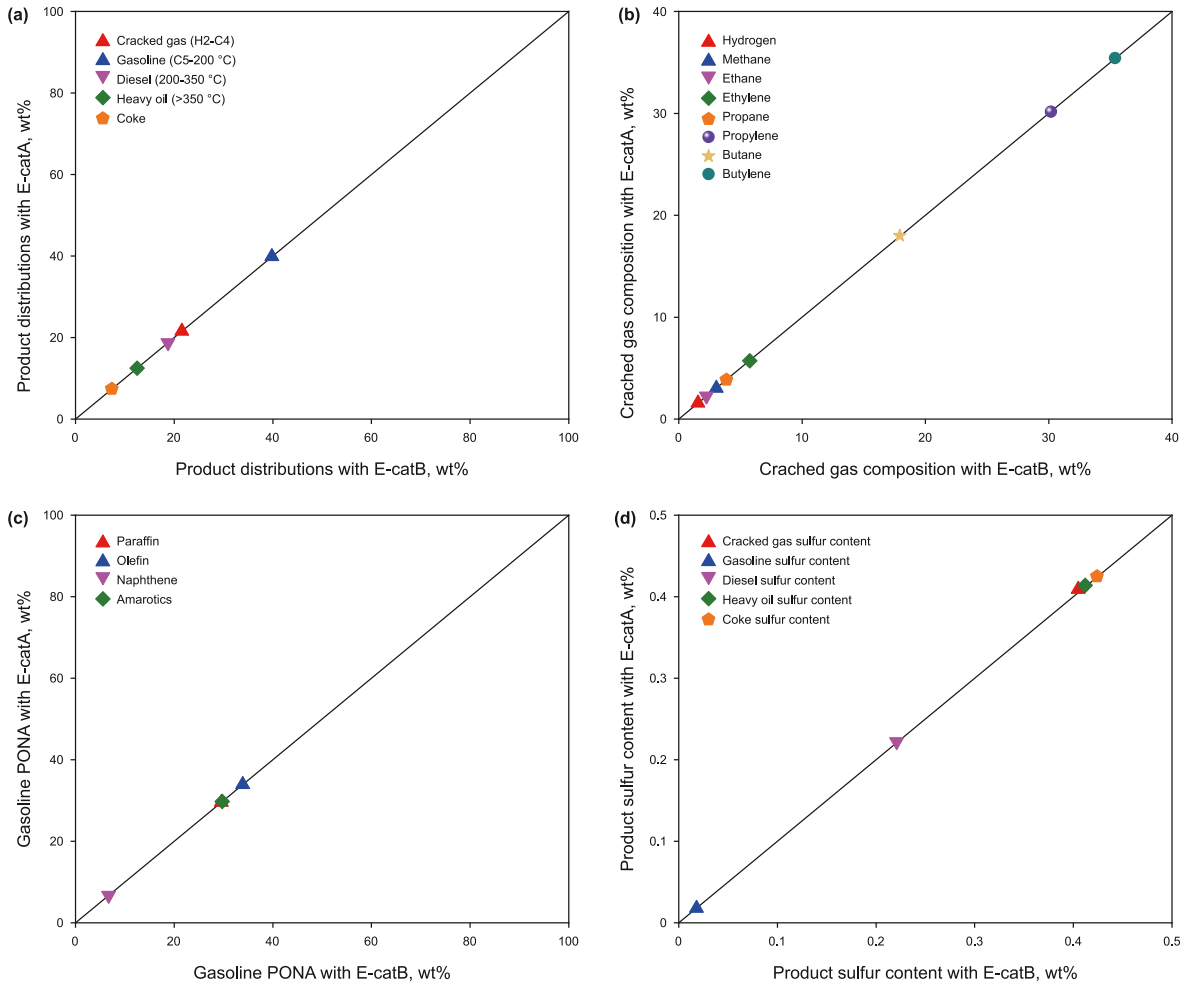


Fig. 10. Parity plots comparing E-catB and E-catA experimental values. **(a)** FCC product distributions, **(b)** FCC cracked gas composition, **(c)** FCC gasoline composition, **(d)** FCC product sulfur content.

reaction time of more than 0.1 s, complete conversion of SO_2 to H_2S can be achieved, with H_2S selectivity reaching 100%. Fig. 11(b)–11(f) shows that as the reaction temperature ranged from 485 to 500 °C, the shortest reaction time required for the complete conversion of SO_2 to H_2S decreased gradually from 0.7 to 0.4 s. This indicates that the conversion of SO_2 to H_2S is fast and that the reaction temperature plays a crucial role. From these findings, it can be inferred that when H_2 is used in the prelift zone (>600 °C), complete conversion of SO_2 to H_2S can occur in more than 0.1 s, and the reaction time is not a limiting factor. In the riser zone (485–500 °C), complete conversion of SO_2 to H_2S can be achieved in a reaction time of more than 0.7 s.

3.4.2. Kinetic modelling

Based on the experimental data presented in Fig. 11, it is evident that in the riser zone (475–500 °C), the complete conversion of SO_2 to H_2S by H_2 within a short reaction time is challenging. Therefore, it becomes necessary to explore the kinetic conversion characteristics and determine the conversion law within this operating range. This information is crucial in guiding the maximization of SO_2 conversion to H_2S. As a result, kinetic modeling of the reduction of SO_2 by H_2 in the riser zone (475–500 °C) was conducted. During the reduction of SO_2 by H_2, H_2S or sulfur can be generated. Hence, the total reaction equation is expressed as:

$$(2+x)H_2 + SO_2 = xH_2S + (1-x)S + 2H_2O \quad (5)$$

Considering that the molar amount of H_2 is significantly greater than that of SO_2, the concentration of H_2 in the kinetic equation is treated as a constant. Consequently, the reaction can be considered a first-order reaction. The corresponding kinetic mathematical equation can be expressed as:

$$\frac{dC_A}{dt} = -KC_A \quad (6)$$

$$C_A = C_{A0}(1 - X_a) \quad (7)$$

Where C_A is the mass concentration of SO_2, t (s) is the reaction time, K (s^{-1}) is the reaction rate constant, C_{A0} is the initial mass concentration of SO_2, and X_a is the conversion of SO_2. Transform the above equations:

$$\ln C_A - \ln C_{A0} = -Kt \quad (8)$$

$$\ln\left(\frac{1}{1-X_a}\right) = Kt \quad (9)$$

The curves of $\ln(1/(1-X_a))$-reaction time are shown in Fig. 12. The corresponding R^2 values for the relevant indexes are all greater

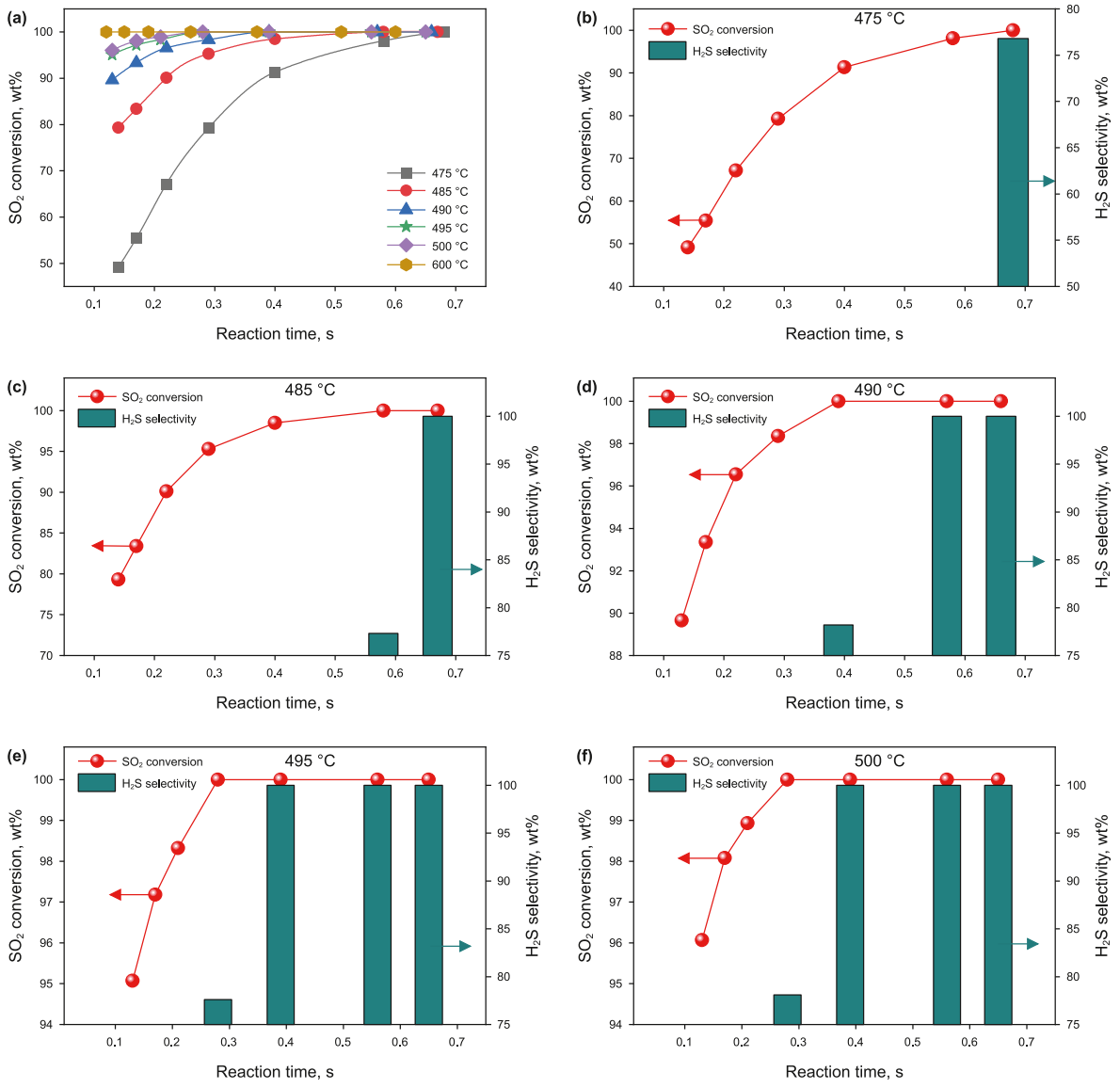


Fig. 11. SO_2 conversion and H_2S selectivity at reaction times of 0.1–0.7 s. **(a)** SO_2 conversion at different temperature, **(b)** SO_2 conversion and H_2S selectivity at 475 °C, **(c)** SO_2 conversion and H_2S selectivity at 485 °C, **(d)** SO_2 conversion and H_2S selectivity at 490 °C, **(e)** SO_2 conversion and H_2S selectivity at 495 °C, **(f)** SO_2 conversion and H_2S selectivity at 500 °C.

than 0.98. The data points in the graph exhibit a significant linear relationship, suggesting that the reaction aligns more closely with the first-order kinetic reaction model. Consequently, the reduction of SO_2 by H_2 in the riser zone (475–500 °C) can be viewed as a first-order reaction. The kinetic rate constants k and the corresponding indices at different temperatures are tabulated in Table 9, with k increasing as the temperature increases.

By utilizing the Arrhenius formula, it is possible to determine the average activation energy (E_a) for the reduction of SO_2 by H_2 at 475–500 °C. The curve of ln K-1000/T is depicted in Fig. 13. The calculations indicate that the E_a of the reaction within the temperature range of 475–500 °C is 263 kJ/mol. Based on the literature, the E_a for the reduction of SO_2 subsequent to the dissociation of H_2 into free radicals is 413.6 kJ/mol. Hence, it can be inferred that the E_a for the reduction of SO_2 by hydrogen with an FCC equilibrium catalyst is lower than 413.6 kJ/mol, indicating that the reduction reaction is more favorable when employing an FCC equilibrium catalyst.

4. Conclusion

In this study, a novel process called FCC-DeSO_x is proposed for the treatment of SO_x using an FCC riser reactor. By utilizing dry gas (rich in H_2), high temperatures, and abundant hydrocarbons in the riser, complete conversion of SO_x to H_2S is achieved. The resulting H_2S, along with the cracked gas, is then subjected to downstream processes to obtain sulfur products. Thermodynamic analysis revealed that the two reaction zones—dry gas prelift and upper zone of the riser—can totally convert SO_x to H_2S, in the lower zone of the riser, H_2S selectivity over 99.98% and sulfur-containing coke selectivity less than 0.02%. The reaction does not affect the catalyst once it reaches thermodynamic equilibrium. However, an increase in SO_x residence time in the riser may lead to the consumption of olefins in the cracked gas and the introduction of elemental sulfur into aromatic rings or coke. A comparison of the magnitudes of the thermodynamic equilibrium constants indicates that higher hydrocarbon carbon numbers and reaction temperatures promote the

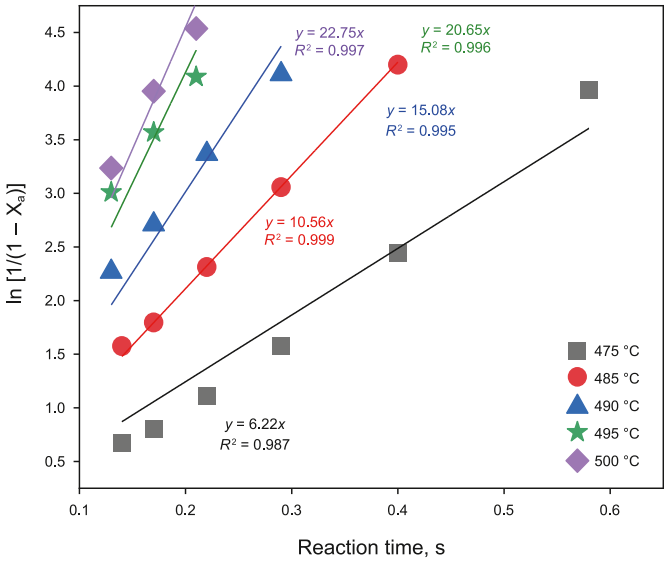


Fig. 12. First-order kinetic rate constant plots of SO_2 reduced by H_2.

Table 9
SO_2 conversion rate constants in the FCC riser zone (475–500 °C).

Temperature, °C	Rate constants, s^{-1}	Relevant index R^2
475	6.22	0.987
485	10.56	0.999
490	15.08	0.995
495	20.65	0.996
500	22.75	0.997

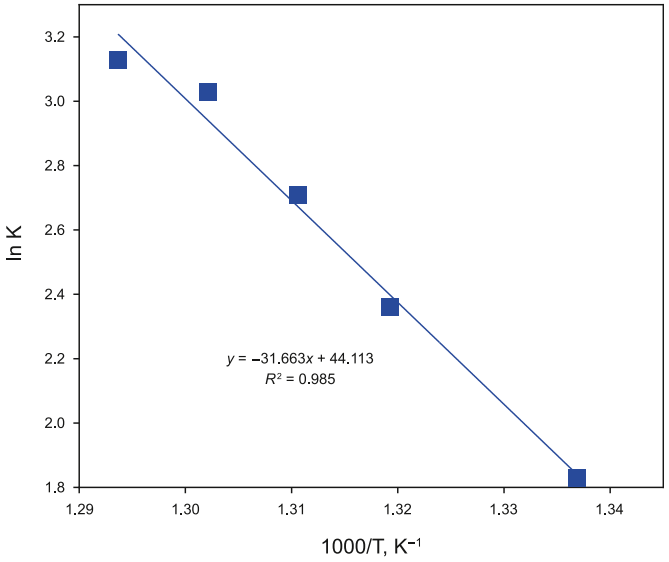


Fig. 13. Arrhenius plots for the SO_2 reduction.

reduction of SO_x to H_2S.

To validate the findings, a simulated experimental investigation on the dry gas reduction of SO_2 was carried out. The results demonstrate that with FCC equilibrium catalyst, 100% H_2S yield could be obtained above 475 °C and over 2.7 s with a reducing gas of H_2, CH_4 and C_2H_6 mixture or H_2. H_2 in the dry gas plays a major role in the SO_2 reduction, while CH_4 and C_2H_6 do not improve the SO_2 conversion or H_2S yield. For the reduction of SO_2 by H_2, FCC equilibrium catalyst exhibits superior H_2S yield compared to fresh FCC catalyst. Process optimization further revealed an optimal H_2/SO_2 molar ratio of 16 when using the FCC equilibrium catalyst. And there was no change in the specific surface area, pore volume and FCC performance of the FCC equilibrium catalysts before and after SO_2 reduction.

Moreover, a study was conducted to investigate the minimum reaction time required for the complete conversion of SO_2 to H_2S under optimal H_2/SO_2 molar ratio conditions. In the dry gas prelift zone, when the reaction temperature exceeds 600 °C, complete reduction of SO_2 to H_2S can be achieved within 0.1 s using H_2. In the riser zone, complete conversion of SO_2 to H_2S occurs more than 0.7 s at reaction temperatures above 485 °C. Based on these observations, a kinetic model was developed for the reduction of SO_2 by H_2, which followed first-order kinetics and had a reaction activation energy of 263 kJ/mol.

CRediT authorship contribution statement

Fa-Lu Dang: Writing – review & editing, Writing – original draft, Formal analysis, Data curation. **Gang Wang:** Writing – review & editing, Supervision, Resources, Methodology, Funding acquisition, Conceptualization. **Jing-Cun Lian:** Formal analysis, Data curation. **Yu Yang:** Formal analysis, Data curation. **Mei-Jia Liu:** Writing – review & editing.

Declaration of competing interest

The authors declare that they have no known competing financial interests or personal relationships that could have appeared to influence the work reported in this paper.

Acknowledgements

This work is supported by General Program of National Natural Science Foundation of China (22178385).

References

Abdulhamid, H., Fridell, E., Dawody, J., Skoglundh, M., 2006. In situ FTIR study of SO_2 interaction with $Pt/BaCO_3/Al_2O_3$ NO_x storage catalysts under lean and rich conditions. J. Catal. 241 (1), 200–210. https://doi.org/10.1016/j.jcat.2006.04.034.

Alotaibi, F.M., González-Cortés, S., Alotibi, M.F., Xiao, T.C., Al-Megren, H., Yang, G.D., Edwards, P.P., 2018. Enhancing the production of light olefins from heavy crude oils: turning challenges into opportunities. Catal. Today 273, 86–98. https://doi.org/10.1016/j.cattod.2018.02.018.

Baillie, C., 2019. FCC additive technology for SO_x reduction. Petrol. Technol. Q. 24 (5), 69–73.

Bejarano, C., Jia, C.Q., Chung, K.H., 2003. Mechanistic study of the carbothermal reduction of sulfur dioxide with oil sand fluid coke. Ind. Eng. Chem. Res. 42 (16), 3731–3739. https://doi.org/10.1021/ie0206711.

Chen, C., Weng, H., 2005. Nanosized CeO_2-supported metal oxide catalysts for catalytic reduction of SO_2 with CO as a reducing agent. Appl Catal B-Environ Energy 55 (2), 115–122. https://doi.org/10.1016/j.apcatb.2004.08.001.

Chen, J.W., Xu, Y.H., 2015. Catalytic Cracking Process and Engineering, vol. 3. China Petrochemical Press, Beijing, pp. 251–284 (in Chinese).

Chen, Y.X., Li, J.G., Li, Y.J., et al., 2020. Comparative study of the flue gas desulfurization using different–grade natural manganese oxides. Chem. Eng. Technol. 43 (2), 337–342. https://doi.org/10.1002/ceat.201900266.

Chen, Z.H., Shang, G.J., Zhang, L., Liu, S.X., Sun, T., Fan, H.L., 2011. Formation of carbonyl sulfide in removal of hydrogen sulfide using metal oxide sorbents. Mod. Chem. Ind. 31 (S1), 244–251. https://doi.org/10.16606/j.cnki.issn0253-4320.2011.s1.074 (in Chinese).

Cheng, W.P., Liang, X.Z., Yang, J.G., He, M.Y., 2009. Structure and properties of MgAlCuFe complex oxide for FCC desulfurization: effect of Fe and Cu contents. Chin. J. Catal. 30 (1), 31–36. https://doi.org/10.1007/s10553-009-0086-x (in Chinese).

Corma, A., Corresa, E., Mathieu, Y., Sauvanaud, L., Al-Bogami, S., Al-Ghrami, M.S., Bourane, A., 2017. Crude oil to chemicals: light olefins from crude oil. Catal. Sci. Technol. 7 (1), 12–46. https://doi.org/10.1039/c6cy01886f.

Doumani, T.F., Deery, R.F., Bradley, W.E., 1944. Recovery of sulfur from sulfur dioxide in waste gases. Ind. Eng. Chem. 36 (4), 329–332. https://doi.org/10.1021/ie50412a011.

Feng, R., Al-Megren, H., Zhang, Z., Al-Kinany, M., Yan, Z.F., Zhang, Z.D., Gao, X.H., 2014. Soft-templating pathway to create nanostructured Mg-Al spinel as high-temperature absorbent for SO_2. J. Porous Mater. 21 (6), 947–956. https://doi.org/10.1007/s10934-014-9843-2.

Feng, T., Zhao, X.Q., Wang, T., Xia, X., Zhang, M.Z., Huan, Q.C., Ma, C.Y., 2016. Reduction of SO_2 with CO to elemental sulfur in activated carbon bed. Energy Fuel. 30 (8), 6578–6584. https://doi.org/10.1021/acs.energyfuels.6b01006.

Gaudin, P., Dorge, S., Nouali, H., et al., 2016. CuO/SBA-15 materials synthesized by solid state grinding: influence of CuO dispersion and multicycle operation on $DeSO_x$ performances. Appl Catal B-Environ Energy 181, 379–388. https://doi.org/10.1016/j.apcatb.2015.08.011.

Ge, C., Yu, X.Z., Liu, M.W., Bai, L., 2023. Development status and future trend of China's sulfur industry. Mod. Chem. Ind. 43 (12), 7–10 (in Chinese).

Ge, T.T., Zuo, C.C., Zhang, J.P., Wei, L.B., Li, C.S., 2018. Selective reduction of SO_2 in smelter off-gas with coal gas to sulfur over metal sulfide supported catalysts. Ind. Eng. Chem. Res. 57 (12), 4170–4179. https://doi.org/10.1021/acs.iecr.8b00213.

Gong, J.Y., 2020. The development of catalytic cracking catalyst industry faces six major challenges. Sinopec Monthly 10, 27–29 (in Chinese).

Gong, W.X., 2022. Technical Question and Answer of Flue Gas Desulfurization, Dust Removal and Denitration in Catalytic Cracking, vol. 2. China Petrochemical Press, Beijing, pp. 31–89 (in Chinese).

Hou, Y.Q., Zhang, R., Han, X.J., Huang, Z.G., Cui, Y., 2017. The mechanism of CO regeneration on V_2O_5/AC catalyst and sulfur recovery. Chem. Eng. J. 316, 744–750. https://doi.org/10.1016/j.cej.2017.02.020.

Hu, D.W., Qing, Y.N., Ma, Z., H, S., 2002. Reduction of sulfur dioxide over transition metal sulfides. Chin. J. Catal. 23 (5), 425–429. https://doi.org/10.1021/cm020635s (in Chinese).

Hu, M., 2012. FCC flue gas emission control technology today and challenges. Sino-Global Energy 17 (5), 77–83 (in Chinese).

Huang, S.B., 2023. Application analysis of "shape change" management cost model of sulfur industrial products. Modern Industrial Economy and Informationization 13 (6), 227–228. https://doi.org/10.16525/j.cnki.14-1362/n.2023.06.076 (in Chinese).

Humeres, E., Moreira, R., Peruch, M., 2002. Reduction of SO_2 on different carbons. Carbon 40 (5), 751–760. https://doi.org/10.1016/S0008-6223(01)00193-2.

Jiang, R.Y., Shan, H.H., Li, C.Y., Nang, C.H., 2011. Preparation and characterization of Mn/MgAlFe as transfer catalyst for SO_x abatement. J. Nat. Gas Chem. 20 (2), 191–197. https://doi.org/10.1016/S1003-9953(10)60171-5.

Jiang, R.Y., Yu, S.L., Zhou, Y.D., Zhu, T., 2016. Study on the relation between the Mn/Al mixed oxides composition and performance of FCC sulfur transfer agent. Catalysts 6 (2), 20–32. https://doi.org/10.3390/catal6020020.

Larraz, R., 2002. Influence of fractal pore structure in claus catalyst performance. Chem. Eng. J. 86 (3), 309–317. https://doi.org/10.1016/S1385-8947(01)00189-9.

Li, B.S., Yuan, S.L., 2014. Synthesis, characterization, and evaluation of TiMgAlCu mixed oxides as novel SO_x removal catalysts. Ceram. Int. 40 (8), 11559–11566. https://doi.org/10.1016/j.ceramint.2014.03.112.

Li, D.N., 2023. Market analysis and research of sulfur industry chain in China. Techno-Economics in Petrochemicals 39 (6), 14–17 (in Chinese).

Li, J., Zhang, L.Q., Zhao, X.Q., et al., 2021. Insights into the effect of regeneration temperature on physicochemical properties and SO_2 removal over powdered activated coke. Fuel 288, 119715. https://doi.org/10.1016/j.fuel.2020.119715.

Li, K.T., Hung, Y.C., 2003. Hydrogenation of sulfur dioxide to hydrogen sulfide over Fe/γ-Al_2O_3 catalysts. Appl. Catal. B Environ. 40 (1), 13–20. https://doi.org/10.1016/s0926-3373(02)00009-7.

Li, P., 2017. Study on desulfurization and denitrification of FCC flue gas. Master, East China University of Science and Technology 2–3 (in Chinese).

Li, X.K., Han, J.R., Liu, Y., Dou, Z.H., Zhang, T., 2022. Summary of research progress on industrial flue gas desulfurization technology. Sep. Purif. Technol. 281, 119849–119870. https://doi.org/10.1016/j.seppur.2021.119849.

Li, Z.L., Zhou, L.S., Wei, Y.H., Peng, H.L., Huang, K., 2020. Highly efficient, reversible, and selective absorption of SO_2 in 1-ethyl-3-methylimidazolium chloride plus Imidazole deep eutectic solvents. Ind. Eng. Chem. Res. 59 (30), 13696–13705. https://doi.org/10.1021/acs.iecr.0c01451.

Liu, Y.X., Shan, Y., Wang, Y., 2020. Novel simultaneous removal technology of NO and SO_2 using a semi-dry microwave activation persulfate system. Environ. Sci. Technol. 54 (3), 2031–2042. https://doi.org/10.1021/acs.est.9b07221.

Luan, H., Lin, J.Y., Xiu, G.L., Ju, F., Ling, H., 2020. Study on compositions of FCC flue gas and pollutant precursors from FCC catalysts. Chemosphere 245, 125528–125534. https://doi.org/10.1016/j.chemosphere.2019.125528.

Magnabosco, L.M., 2007. Principles of the SO_x reduction technology in fluid catalytic cracking units (FCCUs). Stud. Surf. Sci. Catal. 166, 253–305. https://doi.org/10.1016/S0167-2991(07)80199-6.

Miao, R., Dutta, B., 2017. Mesoporous Iron sulfide for highly efficient electrocatalytic hydrogen evolution. J. Am. Chem. Soc. 139 (39), 13604–13607. https://doi.org/10.1021/jacs.7b07044.

GB 31571–32015. Ministry of Ecology and Environment of the People's Republic of China, 2015. Emission standard of pollutants for petroleum chemistry industry. https://www.mee.gov.cn/ywgz/fgbz/bz/bzwb/dqhjbh/dqgdwrywrwpfbz/201505/W020240612353987637486.pdf.

Mirhoseini, H., Taghdiri, M., 2016. Extractive oxidation desulfurization of sulfur-containing model fuel using hexamine–phosphotungstate hybrid as effective heterogeneous catalyst. Fuel 167, 60–67. https://doi.org/10.1016/j.fuel.2015.11.042.

Mousavi, S.E., Pahlavanzadeh, H., Khani, M., Ebrahim, H.A., Mozaffari, A., 2018. Selective catalytic reduction of SO_2 with methane for recovery of elemental sulfur over nickel-alumina catalysts. React. Kinet. Mech. Catal. 124 (2), 669–682. https://doi.org/10.1007/s11144-018-1360-x.

Nie, Y.X., Li, S., Dai, J.F., He, D.D., Mei, Y., 2020. Catalytic effect of Mn^{2+}, Fe^{3+} and Mg^{2+} ions on desulfurization using phosphate rock slurry as absorbent. Chem. Eng. J. 390, 124568–124578. https://doi.org/10.1016/j.cej.2020.124568.

Oloruntoba, A., Zhang, Y., Hsu, C.S., 2022. State-of-the-Art review of fluid catalytic cracking (FCC) catalyst regeneration intensification technologies. Energies 15 (6), 2061. https://doi.org/10.3390/en15062061.

Olson, D.G., Tsuji, K., Shiraishi, I., 2000. The reduction of gas phase air toxics from combustion and incineration sources using the MET-Mitsui-BF activated coke process. Fuel Process. Technol. 65, 393–405. https://doi.org/10.1016/S0378-3820(99)00106-X.

Polato, C., Henriques, C., Rodrigues, A., Monteiro, J., 2008. De-SO_x additives based on mixed oxides derived from Mg,Al-hydrotalcite-like compounds containing Fe, Cu, Co or Cr. Catal. Today 133–135, 534–540. https://doi.org/10.1016/j.cattod.2007.12.046.

Polato, C.M.S., Henriques, C.A., Neto, A.A., Monteiro, J.L.F., 2005. Synthesis, characterization and evaluation of CeO_2/Mg,Al-mixed oxides as catalysts for SO_x removal. J. Mol. Catal. Chem. 241 (1–2), 184–193. https://doi.org/10.1016/j.molcata.2005.07.006.

Stratiev, D., Ivanov, M., Chavdarov, L., Argirov, G., Strovegli, G., 2023. Revamping fluid catalytic cracking unit, and optimizing catalyst to process heavier feeds. Appl. Sci. 13 (3), 2017. https://doi.org/10.3390/app13032017.

Wang, C.L., Xie, Z.Z., Zhao, Y., Zhao, X.G., Wang, L.X., Ren, X., 2019. Simulation study on adsorption and dissociation of hydrogen on iron, platinum and nikel metals. Pet. Process. Petrochem. 50 (2), 50–56 (in Chinese).

Wang, G., 2006. Studies on the Reaction Behavior of Residuum Catalytic Cracking with High Temperature and Short Contact Time. Doctor. China University of Petroleum, Beijing, pp. 86–106 (in Chinese).

Wang, L.Y., Zhang, Y.J., Liu, Y., Xie, H.L., Xu, Y.L., Wei, J.P., 2020. SO_2 absorption in pure ionic liquids: solubility and functionalization. J. Hazard Mater. 392, 122504–122522. https://doi.org/10.1016/j.jhazmat.2020.122504.

Wu, C., 2021. Research on emission characteristics of flue gas pollutants from typical FCC units. Doctor, East China University of Science and Technology 1–8 (in Chinese).

Xia, H., Liu, B.S., Li, Q., Huang, Z.B., Cheung, A.S.C., 2017. High capacity Mn-Fe-Mo/FSM-16 sorbents in hot coal gas desulfurization and mechanism of elemental sulfur formation. Appl. Catal. B Environ. 200, 552–565. https://doi.org/10.1016/j.apcatb.2016.07.053.

Xu, Y.H., Zuo, Y.F., Bai, X.H., Du, L.Y., Han, Y.Y., 2021. Development background,development idea and conceptual design of fcc process for targeted cracking to light olefins. Petroleum processing and petrochemical 52 (8), 1–11 (in Chinese).

Yang, M., Wang, G., Han, J.N., Gao, C.D., Gao, J.S., 2023. Fischer-Tropsch wax catalytic cracking for the production of low olefin and high octane number gasoline: process optimization and heat effect calculation. Petrol. Sci. 20 (2), 1255–1265. https://doi.org/10.1016/j.petsci.2022.08.019.

Yi, H.H., Ma, C.B., 2019. Synthesis of MgO@CeO_2-MnO_x core shell structural adsorbent and its application in reducing the competitive adsorption of SO_2 and NO_x in coal-fired flue gas. Chem. Eng. J. 372, 129–140. https://doi.org/10.1016/j.cej.2019.04.120.

Zawadzki, J., Wisniewski, M., 2007. An infrared study of the behavior of SO_2 and NO_x over carbon and carbon-supported catalysts. Catal. Today 119 (1–4), 213–218. https://doi.org/10.1016/j.cattod.2006.08.037.

Zhang, L.Z., Qin, Y.H., Chen, B.Z., Peng, Y.G., He, H.B., Yuan, Y., 2016. Catalytic reduction of SO_2 by CO over CeO_2–TiO_2 mixed oxides. T Nonferr Metal Soc 26 (11), 2960–2965. https://doi.org/10.1016/s1003-6326(16)64426-6.

Zhao, H.L., Ji, L.J., Zhang, X.J., 2022. Technological progress and market analysis of refined sulfuric acid in China. Sulphuric Acid Industry 9, 7–9 (in Chinese).

Zhou, Y.H., 2020. The development and application of sulfur and its deep processing products before the market. Petrochemical Industry Technology 27 (10), 199–262 (in Chinese).